

CrystEngComm

Accepted Manuscript



This is an *Accepted Manuscript*, which has been through the Royal Society of Chemistry peer review process and has been accepted for publication.

Accepted Manuscripts are published online shortly after acceptance, before technical editing, formatting and proof reading. Using this free service, authors can make their results available to the community, in citable form, before we publish the edited article. We will replace this *Accepted Manuscript* with the edited and formatted *Advance Article* as soon as it is available.

You can find more information about *Accepted Manuscripts* in the [Information for Authors](#).

Please note that technical editing may introduce minor changes to the text and/or graphics, which may alter content. The journal's standard [Terms & Conditions](#) and the [Ethical guidelines](#) still apply. In no event shall the Royal Society of Chemistry be held responsible for any errors or omissions in this *Accepted Manuscript* or any consequences arising from the use of any information it contains.

COMMUNICATION

P-type Cu_7Te_5 Single-crystalline Nanocuboids: Size-Controlled Synthesis and Their Large-scale Self-assembly

Cite this: DOI: 10.1039/x0xx00000x

Received 00th January 2014,
Accepted 00th January 2014

Baosong Dai, Qian Zhao, Jing Gui, Jiatao Zhang*, and Hesun Zhu

DOI: 10.1039/x0xx00000x

www.rsc.org/

Cu_7Te_5 single-crystalline nanocuboids have been synthesized by a low-temperature solvothermal strategy, using environment-friendly chemicals. The size from nanometer to sub-micrometer has been controlled through adjusting the dodecanethiol (DDT) concentration. By DDT capping induced appropriate van der Waals interactions, the alignment of nanocuboids leads to large-scale self-assembly into superstructures or supracrystals. The UV-Vis-NIR spectra of as-prepared nanocuboid colloid exhibited potential LSPR properties. The Mott-Schottky impedance potential curve measurement confirmed the p-type conductivity of as-prepared Cu_7Te_5 Nanocuboids.

1. Introduction

Copper tellurides (Cu_{2-x}Te) nanocrystals (NCs), have composition, size and shape dependent properties, such as near-infrared (NIR) localized surface plasmon resonance (LSPR), thermoelectric and ionic conductivity properties, which have gained potential applications in surface-enhanced Raman scattering (SERS), photothermal conversion, solar cells, and electroconductive electrodes.¹⁻³ It is usually p-type semiconductors because of the presence of copper vacancies. Copper vacancies not only determine charge transport properties but also provide composition-dependent LSPR properties.^{4,5} By adjusting the Cu:Te ratio, Copper tellurides (Cu_{2-x}Te) can exist in a wide range of compositions and phases. Thus, the well-defined composition, shape and uniform size control will be important to control LSPR and transport properties. There are many groups, such as the Tuan, Cabot, Moreels, Feldmann, and Yu groups have studied the synthesis and properties of copper tellurides nanostructures.³⁻⁷ However, the more flexible size control of Cu_{2-x}Te NCs, from nanometer to micrometer, by a facile strategy is still necessary in order to control their optical and electronic properties. There are few reports on the synthesis and properties of Rickardite Cu_7Te_5 NCs.³⁻¹² In this paper, without addition of special precursors, we use environment-friendly common chemicals, copper stearate, trioctylphosphine telluride (TOP-Te), oleic acid (OA) in toluene solvent by low-temperature solvothermal method to synthesize Cu_7Te_5 nanocuboids with flexible size control.

Monodisperse NCs can self-assemble into superstructures under the appropriate conditions of temperature, solvent and coating

agents.¹³ These self-assemblies can exhibit tunable physical and chemical properties, but also lay the foundation for assembly-based optoelectronic nanodevices. The self-assembly of nanocubes by dipole-dipole interaction enabled face-to-face alignment have been researched by the Yang, Xia, and Fang group et.al.¹¹⁻¹⁶ The self-assembly research of nanocuboids have only obtained limited progress because of their flexible anisotropic rectangular shapes.¹⁷ In particular, not only the shape, size of NCs, but also uniform nanogaps between NCs can affect LSPR properties distinctly. Here, by this new synthesis strategy, the good monodispersity, large-scale monolayer, multi-layer self-assembly and different assembling modes of Cu_7Te_5 nanocuboids have been realized. The p-type confirmation and LSPR properties of them have also been investigated.

2. Experimental section

2.1 Copper stearate (CuSt_2) preparation:

All chemicals were used without further further processing. The CuSt_2 was synthesized according to reference.¹⁸ Typically, 2.5 mmol (0.4262 g) $\text{CuCl}_2 \cdot 2\text{H}_2\text{O}$ and 5 mmol (1.5323 g) of sodium stearate were dissolved in a mixture of 10 mL distilled water, 70 mL hexane and 50 mL methanol at 60°C for 4 h. The upper organic layer containing CuSt_2 was decanted and washed for several times. The CuSt_2 in solid form was finally obtained after the total evaporation of residual hexane and methanol.

2.2 Top-Te organic precursor preparation:

1 mmol (0.128 g) Te powder was dissolved in 3 mmol (1.34 mL) TOP at 150 °C under nitrogen for more than 2 h until the Te powder was completely dissolved. Then we get a yellow clear solution and it was diluted by toluene solvent.

2.3 Synthesis of Cu_7Te_5 nanocuboids:

Typically, 0.25 mmol CuSt_2 was dissolved in 5 mL toluene to form a clear solution, then 6 mL oleic acid (OA) was introduced into the solution and 2 mL Top-Te precursor was added. After kept stirring for 5 min, 2 mL dodecanethiol (DDT) was introduced to get a homogeneous solution. Then it was transferred into a Teflon-lined

autoclave with 25 mL capacity. The autoclave was sealed and heated at 150 °C for 1 h. The product was washed by 20 mL methanol for several times.

2.4 Characterizations:

The samples for TEM, electron diffraction characterizations were prepared by adding one drop of toluene colloid with the product onto a 300 mesh nickel grid with carbon support film. Low resolution transmission electron microscopic (LRTEM), JEOL JEM-1200EX working at 100 kV, and high-resolution transmission electron microscopic (HRTEM), FEI Tecnai G2 F20 S-Twin working at 200 kV, were utilized to characterize the morphology, monodispersity, self-assembly and the crystallization details. The SEM images and energy-dispersive spectrometry (EDS) analysis were obtained from the sample on silicon substrate through Hitachi FE-SEM 4800 instrument. The samples for XRD measurement were prepared by adding several drops of concentrated product onto silicon (100) wafers and dried at room temperature. The phases of products were determined by XRD on a Bruker D8 Advance X-ray power diffractometer with $\text{CuK}\alpha$ radiation ($\lambda = 1.5418 \text{ \AA}$). The ultraviolet-visible-near-infrared (UV-Vis-NIR) absorption spectra of Cu_7Te_5 nanocuboids toluene colloids were recorded on a Shimadzu UV3600 UV-Vis-NIR spectrophotometer at room temperature. The p-type confirmation of Cu_7Te_5 nanocuboids was carried out by Mott-Schottky impedance potential curves measurement. It was measured on an IM6e electrochemical workstation (Zahner, Germany) with a standard three-electrode system, namely, the working electrode, the Pt counter electrode, and the Ag/AgCl reference electrode. As-prepared Cu_7Te_5 nanocuboids film (with vacuum drying treatment at 100 °C for 3h) on indium tin oxide (ITO) glass was used as the working electrode. The electrolyte was a 200 ml solution of 0.1M NaOH and 0.1M Na_2S .

3. Results and discussion

As illustrated by the LRTEM images in Figure 1 A and Figure S1, monodisperse nanocuboids with the size of 5.9 nm have been prepared with high purity. The HRTEM image in Figure 1B confirmed the single-crystallinity of nanocuboids. Based on indexing, the distance measured between two adjacent fringes are 0.70 nm and 0.50 nm, which should be assigned to be (002) plane of 0.61nm and (032) plane of 0.45nm. The corresponding fast Fourier transform (FFT) pattern (inset in Figure 1B) contains the diffraction spots from the (0 3 2) and (0 3 0) planes of orthorhombic phase Cu_7Te_5 and it is belong to [1 0 0].¹⁹ In other words, the largest exposed faces of the crystal belong to high-indexed {1 0 0} planes.²⁰ By adjusting the concentration of DDT ligand, flexible size control has been realized. Figure 1C and 1D, the LRTEM and HRTEM images exhibited single-crystalline nanocuboids with the size of about 10-12nm. The indexed lattice spacings and the inserted electron diffraction pattern in Figure 1D are consistent with Figure 1B. Figure 1E showed the size of about 100nm and Figure 1F showed the sub-micrometer size when without DDT addition. With the size increasing, the size range become bigger and the rectangular shape become more anisotropic, finally to be micrometer sized nanoplate shapes. The rhombus shaped nanoplates with large size range in Figure 1F is reasonable because of the orthorhombic crystal phase. The powder XRD pattern of nanocuboids in Figure 2A confirmed the Rickardite phase (JCPDS # 26-1117) again. The EDS pattern of samples on silicon substrate from large-scale SEM analysis in Figure 2B exhibit the Cu:Te ratio of about 1.5, which is concordant with Cu_7Te_5 phase confirmed by the XRD and ED characterizations. The strong Si signal comes from the silicon substrate.

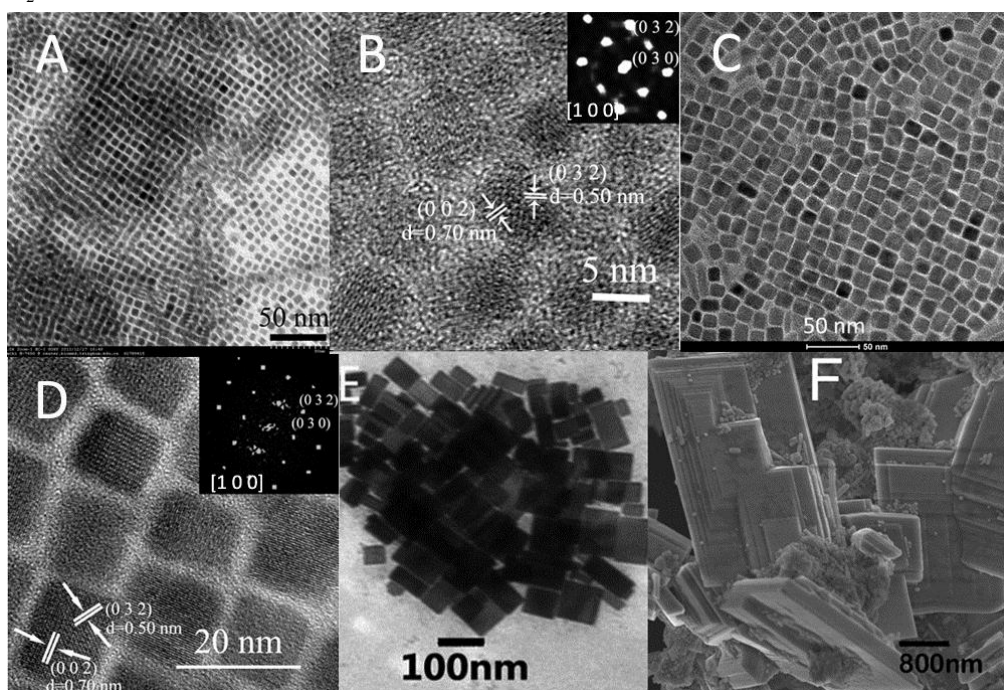


Figure 1 LRTEM and HRTEM morphologies (A-E) and SEM morphology (F) of Cu_7Te_5 nanocuboids from nanometer size to sub-micrometer size. FFT pattern and ED pattern are inserted in Figure B and D.

The advantage of our synthesis method is not only the flexible size control, but also the realization of self-assembly of as-prepared nanocuboids in large scale. In this work, we found that when the size

of as-prepared Cu_7Te_5 nanocuboid is $\sim 5.9\text{nm}$, it is more similar to nanocube and the monodisperse of are good enough. As illustrated by size analysis in Figure 3A, more than 94% of the nanocuboids are

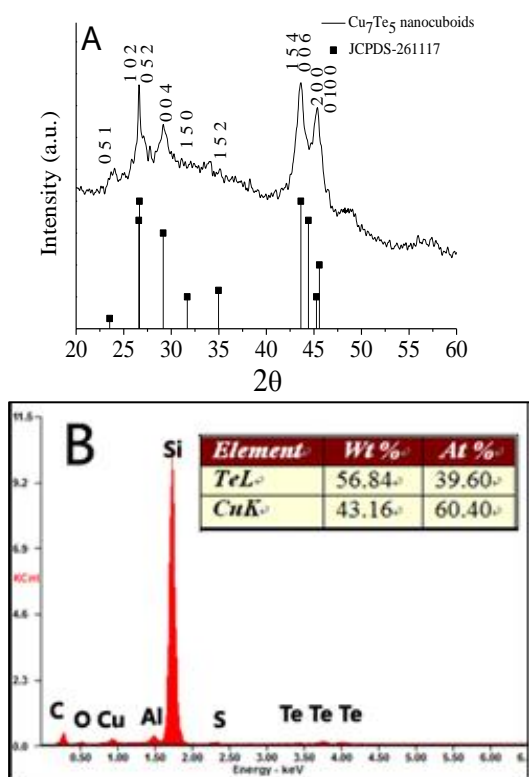


Figure 2 A) XRD pattern of as-prepared Cu₇Te₅ nanocuboids. Bulk Rickardite Cu₇Te₅ (JCPDS #26-1117) is provided for reference and comparison. B) EDS pattern and the Cu:Te ratio by SEM analysis.

in the range of 5.8-6.0 nm. Because of the good monodispersity of nanocuboids and DDT capping which can provide appropriate van der Waals interactions between the nanocrystals,²¹⁻²⁶ the large-scale self-assembly of nanocuboids are realized easily, as shown in Figure 3A, 3B and Figure S2. Here, DDT is one key point to get large-scale self-assembly. Figure 3A exhibited the monolayer self-assembly. The FFT pattern of multi-layer self-assembly (inset in Figure 3B) confirmed the face-to face simple-cubic close packing to be superlattice. As studied by the Glotzer, Yang and Fang group,¹⁴⁻¹⁷ the dipole-dipole interactions promoted face-face alignments. This kind of multi-layer superlattices can be expanded into bulk film scale, as shown in the inserted digital photo in Figure 3B. This large-scale assembly of nanocuboid film will be potential for photothermal and photovoltaic device applications.^{27, 28} The superstructure by hierarchical assembly of nanocuboids was further characterized by scanning TEM (STEM) in Figure 3C. Through DDT capping enabled three-dimensional ordered alignment of nanocuboids, the micrometer-sized superstructures could form (see Figure S3). As the shape evolution in Figure 1, when the size becomes bigger, the anisotropic shape of nanocuboid becomes more and more distinct. Without good monodispersity, the nanocuboid in Figure 1C and E have no long-range-ordered self-assembly. However, the micrometer-sized nanoplates in Figure 1D assemble into superstructures face to face in large scale, as shown in Figure 3D.

LSPR properties in NIR region of Cu_{2-x}Te nanocrystals could be applied in a broad range of fields, from optoelectronics, photothermal therapy, and biomedicine.^{1-4, 27-28} Figure 4A shows the UV-Vis-NIR spectra of colloidal Cu₇Te₅ nanocuboids with two sizes. A strong absorption band centered at 900-1000 nm is clearly observed. It is should attribute to the LSPR of nanocuboids. It was already confirmed that nanocube shape had stronger LSPR than

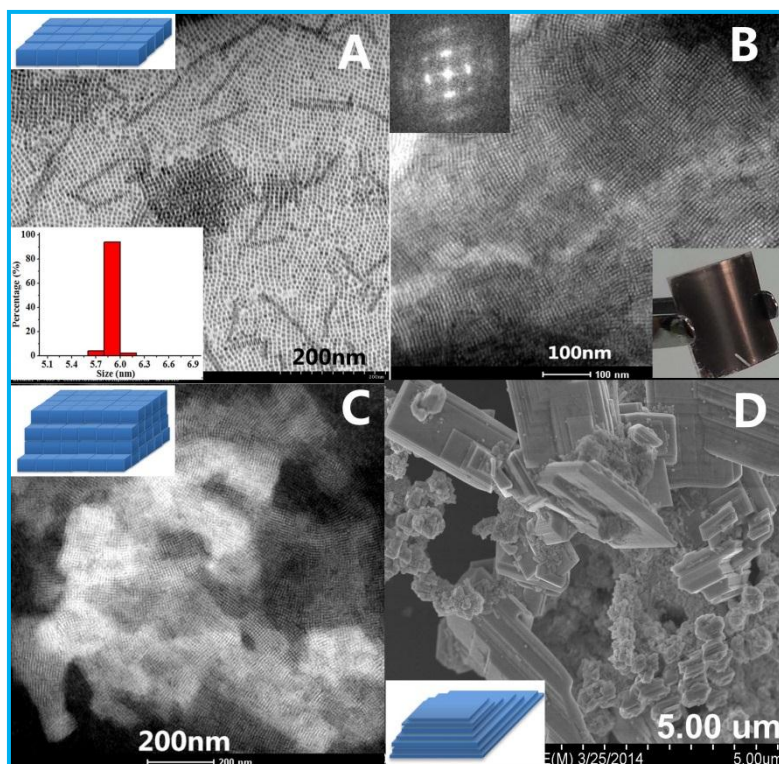


Figure 3 HRTEM and STEM images of monolayer self-assembly (A), large-scale multi-layer superlattice (B, C), large-scale hierarchical assembly of Cu₇Te₅ nanocuboids into superstructures (D). The size analysis of ~5.9 nm nanocuboids is inserted in Figure A. The cartoon inserted in Figure A, C and D is provided to highlight the face-to-face assembly. FFT pattern of assembly and the bulk-sized film on flexible substrate were inserted in Figure B.

COMMUNICATION

nanoplate and nanorod shaped nanocrystals in NIR region.⁴ Therefore, as-prepared monodisperse Cu₇Te₅ nanocuboids which are similar to nanocubes and their self-assembly will be potential for surface enhanced Raman scattering (SERS) detection and photothermal therapy.

P-type Cu_{2-x}Te nanocrystals, due to copper vacancy determined efficient charge transport, are potential for *p/n* heterojunction solar cell application. According to Mott-Schottky equation, for *p*-type semiconductor,²⁹⁻³⁰

$$\frac{1}{C_{sc}^2} = -\frac{2}{\epsilon_0 \epsilon_r N_A A^2} \left(E - E_{FB} - \frac{kT}{e} \right) \quad (1)$$

where C_{sc} is space charge region capacitance, ϵ_0 and ϵ_r are the vacuum and relative dielectric permittivities, A is the surface area of sample in electrolyte, N_D and N_A are the concentration of donors and acceptors, k is the Boltzmann constant, T is the temperature, E is the potential, and E_{FB} is flat band potential. Typical Mott-Schottky plot of Cu₇Te₅ nanocuboid film ($1/C_{sc}^2$ versus applied potential, where C_{sc} means space charge region capacitance) are shown in Figure 4B, from which the *n* or *p*-type conductivity can be identified.³⁰ The negative slope of all the linear parts confirmed the *p*-type conductivity of as-prepared Cu₇Te₅ nanocuboids. Based on this *p*-type confirmation, the potential *p/n* heterojunction solar cell and optoelectronic device applications could be carried out next.

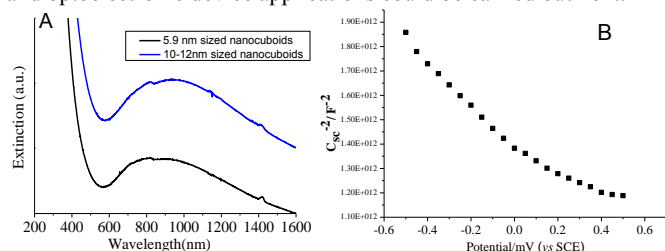


Figure 4 A) UV-Vis-NIR spectra of as-prepared Cu₇Te₅ nanocuboid colloid. B) Typical Mott-Schottky plot of Cu₇Te₅ nanocuboid film in 0.1 M Na₂S and 0.1 M NaOH at 1 kHz. The potentials are measured with respect to standard calomel electrode (SCE).

4. Conclusion

In summary, we developed a low-temperature solvothermal method to synthesize single-crystalline Cu₇Te₅ nanocuboids with flexible size control. Thanks to the DDT capping and the shape uniformity, the dipole-dipole interactions promote the large-scale self-assembly of nanocuboids. The strong LSPR properties in NIR region indicate the potential applications of as-prepared Cu₇Te₅ nanocuboids in sensitive detection and photothermal therapy applications. The *p*-type confirmation of them provides the potential application in photovoltaic devices.

Acknowledgements:

This work was supported by the Natural Science Foundation of China (91123001, 21322105, and 51371015), the funding support from Ministry of Education, China (NCET-11-0793, 2011101120016), and the Program for Beijing Excellent Talents (No. 2012D009011000007).

References:

- J. M. Luther, P. K. Jain, T. Ewers, A. P. Alivisatos, *Nature Materials*, 2011, **10**, 361-366.
- Y. Zhao, C., Burda, *Energy Environ. Sci.* 2012, **5**, 5564-5576.
- I. Kriegel, C. Jiang, J. Rodríguez-Fernández, R. D. Schaller, D. V. Talapin, E. da Como, and J. Feldmann, *J. Am. Chem. Soc.* 2012, **134**, 1583-1590
- W. H. Li, R. Zamani, P. R. Gil, B. Pelaz, M. Ibáñez, D. Cadavid, A. Shavel, R. A. Alvaerz-Puebla, W. J. Parak, J. Arbiol, A. Cabot, *J. Am. Chem. Soc.*, 2013, **135**, 7098-7101.
- H. Yang, C. Chen, F. Yuan, H. Tuan, *J. Phys. Chem. C*, 2013, **117**, 21955-21964.
- I. Kriegel, J. Rodríguez-Fernández, A. Wisnet, H. Zhang, C. Waurisch, A. Eychmüller, A. Dubavik, A. O. Govorov, and J. Feldmann, *ACS Nano*, 2013, **7**, 4367-4377
- J. Liu, J. Xu, H. Liang, K. Wang, S. Yu, *Angew. Chem. Int. Ed.* 2012, **51**, 7420-7425.
- Q. Wang, G. Chen, D. Chen and R. Jin, *CrystEngComm*, 2012, **14**, 6962-6973.
- Y. Zhang, Y. Ni, X. Wang, J. Xia, J. Hong, *Cryst. Growth Des.* 2011, **11**, 4368-4377.
- L. Zhang, Z. Ai, F. Jia, L. Liu, X. Hu, and J. C. Yu, *Chem. Eur. J.* 2006, **12**, 4185-4190.
- H. Shen, X. Jiang, S. Wang, Y. Fu, C. Zhou, L. S. Li., *J. Mater. Chem.*, 2012, **22**, 25050-25056.
- H. B. Li, R. Brescia, M. Povia, M. Prato, G. Bertoni, L. Manna, I. Moreels, *J. Am. Chem. Soc.*, 2013, **135**, 12270-12278.
- M. P. Pileni, *J. Mater. Chem.*, 2011, **21**, 16748-16758.
- J. Henzie, M. Grünwald, A. Widmer-Cooper, P. L. Geissler, P. D. Yang, *Nature Materials*, 2012, **11**, 131-137.
- Z. Quan, H. W. Xu, C. Y. Wang, X. D. Wen, Y. X. Wang, J. L. Zhu, R. P. Li, C. J. Sheehan, Z. W. Wang, D. Smilgies, Z. P. Luo, J. Y. Fang, *J. Am. Chem. Soc.*, 2014, **136**, 1352-1359.
- M. Rycenga, J. M. McLellan, Y. N. Xia, *Adv. Mater.* 2008, **20**, 2416-2420.
- Y. Nakagawa, H. Kageyama, Y. Oaki, H. Imai, *J. Am. Chem. Soc.*, 2014, **136**, 3716-3719.
- S. Li, H. Z. Wang, W. W. Xu, H. L. Si, X. J. Tao, S. Y. Lou, Z. L. Du, L. S. Li, *J. Colloid Interface Sci.*, 2009, **330**, 483-487.
- G. X. Hu, X. Cai, Y. H. Rong, *Fundamentals of Materials Science*, 2th Ed., China, Shanghai Jiao Tong University Press Co., Ltd, 2006, 19-35.
- F.R. Zhou, P.L. Zhu, X.Z. Fu, R.Q. Chen, R. Sun and C.P. Wong, *CrystEngComm*, 2014, **16**, 766-774.
- Z. Zhuang, P. Qing, B. Zhang, Y. D. Li, *J. Am. Chem. Soc.*, 2008, **130**, 10482-10484.
- Q. Zhao, J. T. Zhang, H. S. Zhu, *Prog. Nat. Sci. Mater. Inter.*, 2013, **23**, 588-592.
- X. X. Xu, X. Wang, *J. Mater. Chem.*, 2009, **19**, 3572-3575.
- Z. Zhuang, Q. Peng, X. Wang, Y. D. Li, *Angew. Chem. Int. Ed.*, 2007, **46**, 8174-8177.
- E. V. Shevchenko, D. V. Talapin, N. A. Kotov, S. O'Brien, C. B. Murray, *Nature*, 2006, **40**, 685-689.
- Y. S. Xia, T. D. Nguyen, M. Yang, B. Lee, A. Santos, P. Podsiadlo, Z. Tang, S. C. Glotzer, N. A. Kotov, *Nat.*

- Nanotechnol.*, 2011, **6**, 580-585.
27. Lu, W.; Huang, Q.; Li, C.; Chen, W. *Nanomedicine* 2010, **5**, 1161–1171.
28. C. Lin, W. Lee, M. Lu, S. Chen, M. Hung, T. Chan, H. Tsai, Y. Chueh* and L. Chen, *J. Mater. Chem.*, 2012, **22**, 7098-7100.
29. D. F. Underwood, T. Kippeny, S. J. Rosenthal, *J. Phys. Chem. B* 2001, **105**, 436-440.
30. A. Izgorodin, O. Winther, B. Winther, D. R. MacFarlane, *Phys. Chem. Chem. Phys.* 2009, **11**, 8532-8536.

Research Center of Materials Science, School of Materials Science & Engineering, Beijing Institute of Technology, Beijing 100081, PR China

*Corresponding author: Beijing Institute of Technology, Beijing 100081, China. Tel.: +86 10 68918065; Fax: +86 1068918065. E-mail: zhangjt@bit.edu.cn.

† Footnotes should appear here. These might include comments relevant to but not central to the matter under discussion, limited experimental and spectral data, and crystallographic data.

Electronic Supplementary Information (ESI) available: [FigureS1-Figure S3 and the analysis of the largest exposed faces of the crystal]. See DOI: 10.1039/c000000x/